


An Integrated Approach for Targeting Critical Source Areas to Control Nonpoint Source Pollution in Watersheds

Subhasis Giri¹ · Zeyuan Qiu¹  · Tony Prato² · Biliang Luo³

Received: 12 August 2015 / Accepted: 23 August 2016 /
Published online: 1 September 2016
© Springer Science+Business Media Dordrecht 2016

Abstract This study presents an integrated approach for targeting critical source areas (CSAs) to control nonpoint source pollution in watersheds. CSAs are the intersections between hydrologically sensitive areas (HSAs) and high pollution producing areas of watersheds. HSAs are the areas with high hydrological sensitivity and potential for generating runoff. They were based on a soil topographic index in consistence of a saturation excess runoff process. High pollution producing areas are the areas that have a high potential for generating pollutants. Such areas were based on simulated pollution loads to streams by the Soil and Water Assessment Tool. The integrated approach is applied to the Neshanic River watershed, a suburban watershed with mixed land uses in New Jersey in the U.S. Results show that several land uses result in water pollution: agricultural land causes sediment, nitrogen and phosphorus pollution; wetlands cause sediment and phosphorus pollution; and urban lands cause nitrogen and phosphorus pollution. The primary CSAs are agricultural lands for all three pollutants, urban lands for nitrogen and phosphorus, and wetlands for sediment and phosphorus. Some pollution producing areas were not classified into CSAs because they are not located in HSAs and the pollutants generated in those areas are less likely to be transported by runoff into streams. The integrated approach identifies CSAs at a very fine scale, which is useful for targeting the implementation of best management practices for water quality improvement, and can be applied broadly in different watersheds to improve the economic efficiency of controlling nonpoint source pollution.

✉ Zeyuan Qiu
zeyuan.qiu@njit.edu

¹ Department of Chemistry and Environmental Science, New Jersey Institute of Technology, University Heights, Newark, NJ 07102, USA

² Department of Agricultural and Applied Economics, University of Missouri-Columbia, Columbia, MO 65211, USA

³ College of Economics and Management, Huanan Agricultural University, Guanzhong, Guangdong 510642, China

Keywords Hydrologically sensitive areas · Pollution generating areas · Critical source areas · Soil topographic index · Soil and water assessment tool · Neshanic river watershed

1 Introduction

Nonpoint source (NPS) pollution is a major contributor to water pollution and the degradation of aquatic ecosystems in the United States (Diebel et al. 2008; USEPA 2009). The challenge in reducing NPS pollution is to identify the source of pollutants originating from spatially diverse areas (Carpenter et al. 1998). A targeting approach for reducing agricultural NPS pollution has received considerable attention (e.g., Trevisan et al. 2010; Zhou and Gao 2011; Kaini et al. 2012; Ghebremichael et al. 2013). In particular, there is growing interest in reducing NPS pollution by implementing best management practices (BMPs) in critical source areas (CSAs) (Qiu 2009; White et al. 2009; Giri et al. 2012; Buchanan et al. 2013; Kumar and Mishra 2015).

CSAs are the areas of watersheds where hydrologically sensitive areas (HSAs) and pollution generating areas intersect and which have a high propensity to generate runoff and pollutants (Walter et al. 2000; Qiu 2009; Ghebremichael et al. 2013). CSAs of watersheds have the potential to generate significant pollution loads that can adversely impact the water quality of receiving waterbodies (Srinivasan and McDowell 2009; Shen et al. 2011). Identification and prioritization of CSAs for BMP implementation can mitigate NPS pollution efficiently and cost-effectively while minimizing landscape disturbance (Qiu 2009).

Different approaches have been used to identify watershed areas that disproportionately contribute to NPS pollution. Shen et al. (2015) used the Soil and Water Assessment Tool (SWAT) and statistical analysis to identify and prioritize management areas for controlling total phosphorus concentration in the Daning River watershed located in Hubei, China. Buchanan et al. (2013) used a travel time phosphorus index approach to identify phosphorus CSAs in an agricultural watershed in central New York and found that man-made agricultural ditches are the CSAs for phosphorus in that watershed. Their travel time-phosphorus index approach integrates the probability of runoff generation, topographic position, hydrologic connectivity, and land use to locate CSAs. Thompson et al. (2012) developed an export coefficient to measure the effect of overland flow connectivity on nutrient transport and used that coefficient to identify CSAs for reducing diffuse phosphorus loss in the County Down watershed in Northern Ireland. Shen et al. (2011) applied an agricultural pollution potential index to identify CSAs for reducing nitrogen and phosphorus loads to streams in the Fujiang watershed in Qinghai, China. That study found that as the percentage of agricultural land in CSAs increases, nitrogen and phosphorus loads to streams in the watershed increase. Qiu (2009) used a soil topographic index (STI) to identify CSAs for conservation buffer planning and riparian restoration in Raritan River Basin, New Jersey. Other methods used to identify CSAs include a tiered approach for phosphorus (Doody et al. 2012), a geographical allocation approach for phosphorus (Diebel et al. 2008), and the universal soil loss equation for sediment and phosphorus (Sivertun and Prange 2003; Pandey et al. 2007; Chen et al. 2011). In contrast to this study, which uses two criteria to identify CSAs for watersheds, the above studies use only one criterion.

This study integrates an STI and SWAT to identify CSAs for sediment, nitrogen, and phosphorus at a fine spatial scale. Specific objectives of this study are to: (1) determine HSAs using an STI; (2) identify and characterize pollution producing areas at a fine scale using SWAT; and (3) identify CSAs for sediment, nitrogen, and phosphorus defined as the

intersection of HSAs and high pollution producing areas. This integrated method presented here allows CSAs to be identified at a fine spatial scale, which is useful when implementing BMPs for controlling NPS pollution.

2 Materials and Methods

2.1 Study Area

The study area is the 142 km² Neshanic River watershed (hydrologic unit code-HUC 02030105030), a suburban watershed with mixed land uses located in Central New Jersey in the U.S. (Fig. 1). This watershed is a headwater watershed to the South Branch of the Raritan River that flows eastward and drains into the Atlantic Ocean. The land cover/use for the watershed is 38 % forest, 31 % agriculture, 25 % urban, and the remainder in wetland, water, and barren areas. Major crops grown in the watershed are hay, pasture, corn, and soybeans. Minor crops include winter wheat, rye, and oats. The watershed has a maximum elevation of approximately 209 m and a minimum elevation of 20 m above the mean sea level.

Higher elevations are generally found on the watershed boundary except on the northeast side. Water in the streams flows eastward and drains into the South Branch of the Raritan River. The region where the watershed is located has a humid climate with hot humid summers and cold winters. The highest temperatures in the study area are 27 °C to 30 °C, and the lowest

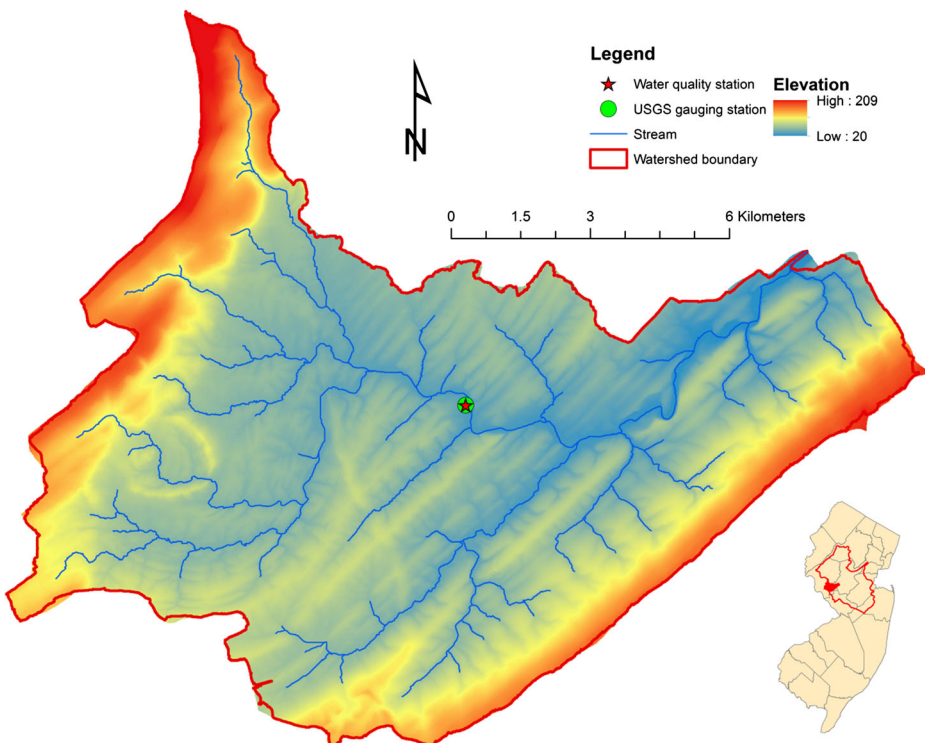


Fig. 1 Topography and location of the Neshanic River watershed in New Jersey

temperatures are $-5\text{ }^{\circ}\text{C}$ to $-7\text{ }^{\circ}\text{C}$. Average mean annual precipitation in the watershed is 1218 mm according to the National Climatic Data Center. Streams in the watershed are classified as FW2 and NT streams. Water in FW2 streams can be used only for industrial purposes and agricultural irrigation; and water in NT streams does not support trout production and maintenance (NJDEP 2011). Water quality in the watershed is impaired due to excessive sediment, phosphorus, and pathogen loads to the streams (Qiu and Wang 2014).

2.2 SWAT Model Description

SWAT was used to characterize the source areas that contribute sediment, nitrogen, and phosphorus loads to streams in the Neshanic River watershed. SWAT is a physically-based, spatially-distributed, watershed scale model developed by the Agricultural Research Service (ARS) of the U.S. Department of Agriculture (USDA) (Arnold et al. 1998). SWAT divides the watershed into several subbasins based on topography. Each subbasin is further delineated into hydrologic response units (HRUs) that have a unique combination of land use, soil, and slope representing diverse natural resource conditions and their responses to management decisions. In this application, the Neshanic River watershed is divided into 6363 HRUs within 115 subbasins.

2.3 Data Sources for SWAT Model

The topography of the Neshanic River watershed is represented by a light detection and ranging (LiDAR) digital elevation model (DEM) at a 3-m resolution that was obtained from the New Jersey Department of Environmental Protection (NJDEP). This study uses composite land use data for the watershed developed from two sources: 2007 land use/cover data developed from aerial photos developed by NJDEP; and a 2013 crop data layer derived from LANDSAT satellite images processed by the USDA National Agricultural Statistics Service (NASS 2014). The NJDEP land use/cover data has more accurate land use/cover classes, but lacks detailed classification of agricultural land. The NASS crop data layer was used to identify cropping patterns within agricultural lands classified using NJDEP data. Soil survey geographic (SSURGO) soil data for the watershed was downloaded from the USDA Natural Resources Conservation Service (NRCS) Geospatial Data Gateway.

Daily streamflow obtained from USGS gauging station 01,398,000 (Fig. 1) was used to calibrate and validate the streamflow simulated by SWAT. Water quality data on sediment, nitrogen, and phosphorus for the same station were downloaded from EPA STORET and National Water Quality Monitoring Council. Daily precipitation and temperature data from the Flemington and Wertsville weather stations were downloaded from the National Climatic Data Center website. The Flemington weather station is just beyond the boundary of the watershed and the Wertsville weather station is located within the watershed. The weather generator embedded in SWAT was used to generate the remaining meteorological data needed for modeling (i.e., wind speed, solar radiation, and relative humidity).

Agricultural management practices for the crops evaluated in the study (i.e., corn, soybeans, winter wheat, oat, rye, pasture, hay, and lawn management) are the typical agricultural practices for these crops used by producers in the study area. The scheduling of tillage, fertilizer application, planting, and harvesting operations were developed in consultation with local producers and NRCS staff in the study area. Crop yields for corn, soybeans, wheat, and hay were downloaded from the USDA NASS website and used to calibrate SWAT's crop growth module.

2.4 Sensitivity Analysis and Model Calibration

A sensitivity analysis was used to identify critical model parameters that have a major influence on streamflow, sediment, nitrogen, and phosphorus. Sensitivity analysis was performed using the Latin-hypercube-one-factor-at-a-time (LH-OAT) method embedded in the SWAT model. Critical model parameters for each water quality constituent identified in the sensitivity analysis were used to calibrate and validate the SWAT model based on a daily time step for simulated streamflow, and sediment, nitrogen, and phosphorus delivery to streams in the watershed. A two-year, warm-up period was used in calibrating model parameters. The model calibration period was 2010–2011 and the validation period was 2012–2013. The Nash-Sutcliffe efficiency (NSE), root mean square error (RMSE)-observations standard deviation ratio (RSR), and percent bias (PBIAS), were used to evaluate how well the SWAT model simulated streamflow and water quality (Moriassi et al. 2007). NSE is a normalized statistic that determines the relative magnitude of the residual variance compared to the measured data variance (Nash and Sutcliffe 1970). PBIAS measures the average tendency of the simulated data to be larger or smaller than their observed counterparts (Gupta et al. 1999). RSR is the ratio of the RMSE and standard deviation of measured data (Singh et al. 2004). The lower RSR indicates the better model performance.

2.5 Deriving HSAs

2.5.1 Soil Topographic Index

STI approximates the propensity of a point in a watershed to generate runoff when variable source hydrology is the dominant watershed hydrological process (Walter et al. 2000). STI for each grid in the watershed was estimated using the following equation (Walter et al. 2000; Qiu 2009):

$$STI = \ln\left(\frac{a}{\tan(\beta)}\right) - \ln(K_s D), \quad (1)$$

where α is the upslope contributing area per unit contour length (m), β is the local surface slope (mm^{-1}), K_s is saturated hydraulic conductivity (m/day), and D is the depth to restrictive layer (m). The first term is a wetness index (see section 2.5.2) and the second term is soil transmissivity (see section 2.5.3). The STI value and the potential for runoff generation are directly related (i.e., the higher the STI value, the greater the likelihood of runoff).

2.5.2 Wetness Index

The wetness index is derived from the 3-m LiDAR DEM obtained from the NJDEP. Using such a fine-scale LiDAR DEM significantly increases the accuracy of the soil topographic index (Buchanan et al. 2014). The wetness index was created in R platform using the R-SAGA package (Brenning 2007). Any depressions in the original LiDAR DEM were filled to create a filled DEM with a smooth surface for analysis following the fill sinks procedure developed by Wang and Liu (2006). The slope of each grid was calculated using the least-squares fitted plane method (Horn 1981; Costa-Cabral and Burges 1996). Catchment area was determined using the multiple triangular flow direction method (Seibert and McGlynn 2007).

2.5.3 Soil Transmissivity

The calculation of soil transmissivity was based on the procedure developed by Hong and Swaney (2007). Soil transmissivity is the product of saturated hydraulic conductivity and depth to a restrictive layer. The latter was extracted from the SSURGO soil database downloaded from the Geospatial Data Gateway of USDA-NRCS. The saturated hydraulic conductivity used to calculate soil transmissivity is the geometric mean of the saturated hydraulic conductivities associated with multiple soil layers above the restrictive layer (Qiu 2009). Soil transmissivity was multiplied by 0.000864 to convert the units of measurement for soil transmissivity to m^2/day .

2.5.4 Hydrologically Sensitive Areas (HSAs)

The wetness index and soil transmissivity were combined in the R-platform to calculate STIs for the watershed. HSAs are a subset of grids that actively generate runoff (i.e., grids with higher STI values in the watershed) (Qiu 2009). HSAs can be defined using various criteria. A simple way to create HSAs is to select a threshold value of STI and define HSAs as areas with STI values that equal or exceed that threshold. In this study, a threshold value of 10 was chosen following the recommendation by Qiu (2009). Hence, HSAs are areas with STIs greater than or equal to ten. HSAs based on this definition covered about 25.5 % of the watershed, which is slightly larger than the management goal of 20 % recommended by Herron and Hairsine (1998).

2.6 Identifying Pollution Producing Areas

The pollution producing area for sediment, nitrogen, and phosphorus was based on the SWAT-simulated pollutant loads per unit area (Tuppad and Srinivasan 2008; Giri et al. 2012). Previous studies identified pollution producing areas for subbasins. This study identified pollution producing areas for HRUs within subbasins of the watershed.

Based on the pollutant loads for HRUs simulated using SWAT, high, medium, and low potential pollution producing areas were delineated using the natural break methods of classification embedded in the ArcGIS platform. The natural break method classifies data into natural groups by minimizing the variance within each group variance while maximizing the variance of between the group means. High potential pollution producing areas for each pollutant were used to determine CSAs.

2.7 Identifying Critical Source Areas

CSAs are watershed areas where pollution source and transport coincide (Walter et al. 2000). In particular, CSAs are areas in the watershed that can have the potential to generate significant amounts of pollutants and are prone to runoff generation through a saturation-excess hydrological process. In this study, CSAs for each pollutant were identified based on the HSAs for the watershed, which were determined using the STIs discussed in section 2.5, and the high potential pollution producing areas for HRUs, which were identified using the SWAT model discussed in section 2.6.

3 Results and Discussions

3.1 SWAT Model Calibration and Validation

Table 1 presents the three model evaluation parameters (i.e., NSE, PBIAS, and RSR) for the model calibration and validation periods and four water constituents (i.e., daily streamflow, sediment, nitrogen, and phosphorus) for the Neshanic River watershed. The calibration period is 2010–2011, the validation period is 2012–2013, and the overall period is 2010–2013 with one exception. The validation for phosphorus was done by using the observations in the overall period due to limited observation on phosphorus concentrations during the validation period. Based on Moriasi et al. (2007), the SWAT model is good when simulating streamflow (NSE = 0.67, RSR = 0.58, and PBIAS = 9.25), very good when simulating sediment (NSE = 0.78, RSR = 0.45, and PBIAS = 2.34) and nitrogen (NSE = 0.76, RSR = 0.47, and PBIAS = 25.34), and satisfactory when simulating phosphorus (NSE = 0.45, RSR = 0.70, and PBIAS = 60.42).

Figure 2 presents hydrographs for observed and simulated streamflow in the watershed during the calibration and validation periods. Observed and simulated streamflow are similar except for several days when the observed streamflow is significantly higher than the simulated streamflow. The Neshanic River watershed has experienced substantial urban development, which has increased the area of impervious surface. This makes the Neshanic River watershed flashier than traditional agricultural watersheds. It appears SWAT is not able to fully capture such flashiness in watershed hydrology.

Some parameters for the watershed, including the radiation use efficiency or biomass energy ratio and the harvest index for primary crops (i.e., corn, soybeans, wheat, and hay), were calibrated to ensure that simulated crop yields match average crop yields for Hunterdon County where the Neshanic River watershed is located. Average crop yields for Hunterdon County were obtained from NASS.

Table 1 Model evaluation parameters for four water constituents in the model calibration and validation periods, the Neshanic River watershed

Constituent	Evaluation parameters	Overall period (2010–2013)	Calibration period (2010–2011)	Validation period (2012–2014)
Flow	NSE	0.67	0.69	0.44
	PBIAS	9.25	9.89	7.82
	RSR	0.58	0.55	0.75
Sediment	NSE	0.78	0.75	0.81
	PBIAS	2.34	-14.63	20.26
	RSR	0.45	0.49	0.43
Nitrogen	NSE	0.76	0.79	0.60
	PBIAS	25.34	31.99	13.15
	RSR	0.47	0.45	0.63
Phosphorus	NSE	0.45	0.57	0.45
	PBIAS	60.42	63.55	60.42
	RSR	0.70	0.65	0.70

NSE is Nash-Sutcliffe efficiency, PBIAS is percent bias, and RSR is root mean square error (RMSE)-observations standard deviation ratio

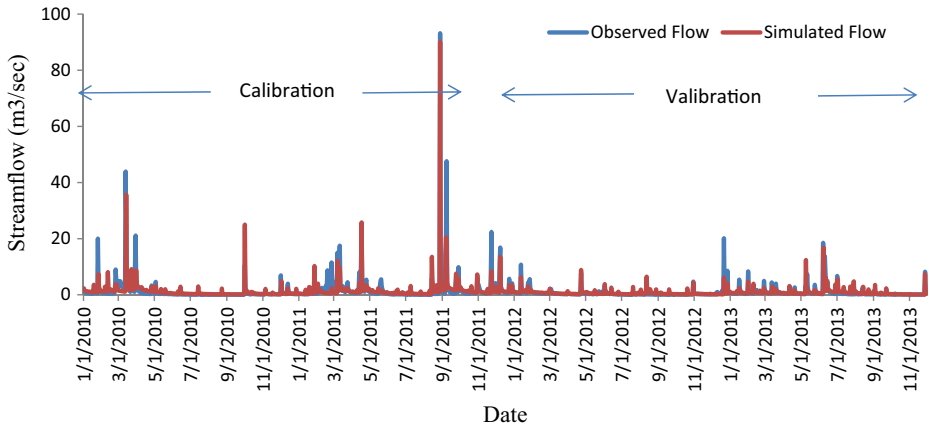


Fig. 2 Observed and simulated streamflow at USGS gauging station 01,398,000 in the Neshanic River watershed

3.2 Hydrologically Sensitive Areas

Soil transmissivity for the watershed varies from $-0.52 \text{ m}^2/\text{d}$ to $0.87 \text{ m}^2/\text{d}$. A negative soil transmissivity index indicates that water infiltration is negligible (Machiwal et al. 2006) and a positive soil transmissivity index indicates that water infiltration is sufficient to reduce the probability of runoff. The estimated values of STI range from 3 to 28 (Fig. 3a). The higher STI (darker shading) indicates the higher probability of runoff generation. During a rainfall event, runoff would first occur in areas with high STI values (Qiu 2009; Lyon et al. 2004).

The delineated HSAs have STI values ranging from 10 to 28. Figure 3b shows the location of HSAs in the watershed, or areas of the watershed that are most prone to producing runoff. HSAs are usually located near streams in the upland areas of the watershed. The total area of HSAs is 3628 ha, which is about 25 % of the watershed. Of the 3628 ha of HSAs, 1291 ha are agricultural lands, 857 ha are forest lands, 812 ha are urban land, 599 ha are wetlands, 65 ha are water, and 4 ha are barren land (Table 2).

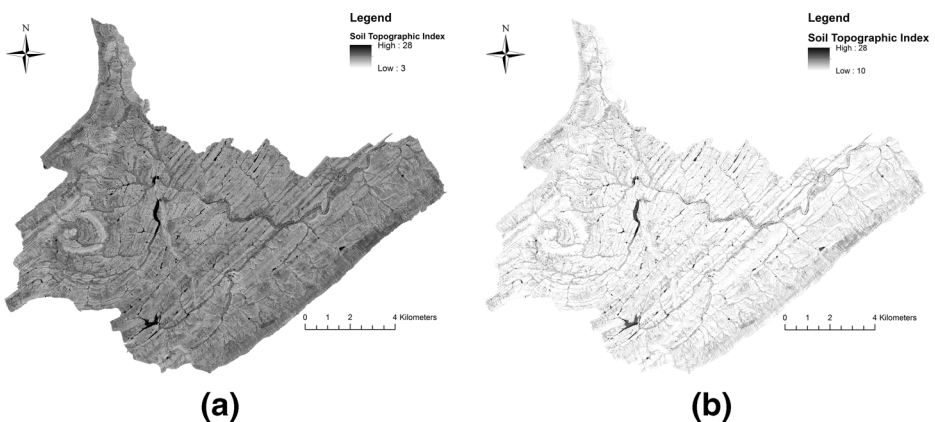


Fig. 3 Soil topographic index (a) and hydrologically sensitive areas (b) for the Neshanic River watershed

Table 2 Land use in hydrologically sensitive areas, high potential pollution producing areas, and critical source areas for sediment, total nitrogen, and total phosphorus, in hectares, the Neshanic River watershed

Land use type	Hydrol. sensitive areas ^a	High potential pollution producing areas ^b			Critical source areas ^c		
		Sediment	TN	TP	Sediment	TN	TP
Ag. land	1290.80	120.85	7.58	627.16	24.48	1.78	145.62
Urban	811.82	0.53	1.61	26.91	0.09	0.62	9.94
Forest	857.29	3.06	0.04	3.73	0.55	0.02	0.76
Wetland	599.11	19.42	0.21	34.53	5.59	0.04	10.89
Barren land	4.15	0.02	0.00	0.02	0.00	0.00	0.00
Water	64.88	1.09	0.00	1.11	0.15	0.00	0.15
Total	3628.04	144.98	9.44	693.47	30.86	2.46	167.38

The areas of various land uses in this table were based on the 2007 NJDEP land use data. The small numbers for some land uses in high potential pollution producing areas and critical source areas, especially the areas less than one hectare, might be caused by the approximation of the physical boundary of HRUs using the NASS crop data layer and inherent inconsistency between the NASS crop data layer and NJDEP land use data. Consequently, these small numbers are not meaningful

^a Estimated based on application of STI

^b Estimated based on application of SWAT

^c Estimated based on the integrated application of STI and SWAT

3.3 Pollution Producing Areas

The pollution producing areas for sediment, nitrogen, and phosphorus in the watershed are based on the SWAT-simulated pollutant loads for HRUs (see Fig. 4). Physical boundaries for HRUs were approximated using the NASS crop data layer as described above.

3.3.1 Sediment Producing Areas

Simulated sediment loads in the watershed range from 0 to 10.20 t/ha (Fig. 4a). Areas with sediment loads between 0 and 0.51 t/ha (tan color), 0.52 and 2.08 t/ha (light brown color), and 2.09 and 10.20 t/ha (dark brown color) are classified as having low, medium, and high potential for producing sediment, respectively. High potential sediment producing areas are concentrated in the central and southeast regions of the watershed, cover 145 ha, and are predominantly agricultural lands (121 ha) and wetlands (19.5 ha) (see Table 2). Medium

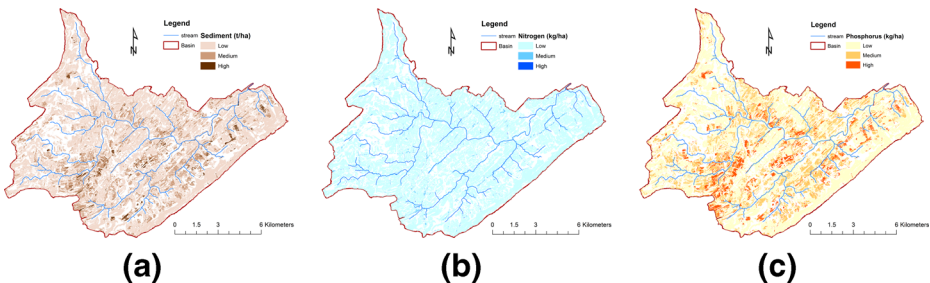


Fig. 4 High, medium, and low potential pollution producing area for sediment (a), nitrogen (b), and phosphorus (c) in the Neshanic River watershed

potential sediment producing areas are concentrated in the central and southern parts of the watershed, which are primarily grass and pasture land. Low potential sediment producing areas are concentrated in the northwest region and the edge of southeast region of the watershed, which are dominated by forests. The results are consistent with other studies. Miller et al. (2011) found that agricultural land contributes significantly to higher suspended solid concentrations in the Lower Kaskaskia River watershed in Illinois. Gyawali et al. (2013) found that agricultural land contributes significantly to sediment load in the U-Tapao River Basin in Thailand. Wilson and Weng (2010) concluded that agricultural land accounts for the highest suspended solid concentration in the Lake Calumet watershed in the Greater Chicago area.

3.3.2 Nitrogen Producing Areas

Nitrogen loads in the watershed vary from 0 to 655 kg/ha (see Fig. 4b). Areas with nitrogen loads between 0 kg/ha and 42.79 kg/ha (light blue color) are classified as low potential nitrogen producing areas, 42.80 kg/ha and 138.04 kg/ha (medium blue color) as medium potential nitrogen producing areas, and 138.05 kg/ha and 654.59 kg/ha (dark blue color) as high potential nitrogen producing areas (see Fig. 4b). The majority of the watershed contains low potential nitrogen producing areas; a very small portion of the watershed contains medium and high potential nitrogen producing areas. The watershed has only 9.44 ha of high potential nitrogen producing areas. Of that area, 7.58 ha are agricultural land and 1.61 ha are urban land (see Table 2). Corroborating results were obtained in other studies. Zampella et al. (2007) found that agricultural and urban land uses contributed significantly to nitrogen concentration in the Mullica River Basin located in the New Jersey Pinelands. Hayakawa et al. (2006) determined that agricultural and urban lands were the primary sources of nitrogen in the Akkeshi and Shibetsu catchments in Japan.

3.3.3 Phosphorus Producing Areas

Low, medium, and high potential phosphorus producing areas are areas having phosphorus loads ranging from 0 to 1.45 kg/ha (yellow color), 1.46 to 3.69 kg/ha (light orange color), and 3.70 to 13.18 kg/ha (dark orange color), respectively (see Fig. 4c). The spatial patterns of phosphorus and sediment producing areas are similar because of the close correlation between sediment and phosphorus loads (i.e., phosphorus attaches to sediment). High potential producing areas for phosphorus cover 693.5 ha of which 627 ha are agricultural land, 27 ha are urban, and 34.5 ha are wetlands (see Table 2). Similar to the high potential producing areas for sediment, agricultural land accounts for the bulk of the phosphorus loads to streams in the watershed, which is consistent with other studies. Pratt and Chang (2012) found that urban and agricultural lands account for the majority of phosphorus loads to streams near the Portland, Oregon metropolitan area. Wan et al. (2014) observed that agricultural and urban lands are the major sources of phosphorus loads to the Lake Tai Basin in China. Some wetlands contribute to phosphorus loads because some of the accumulated nutrients in wetlands are slowly released to receiving waterbodies. Ardon et al. (2010) observed that a restored wetland released more total phosphorus and soluble reactive phosphorus per ha to receiving waterbodies than agricultural land in Albemarle Peninsula in North Carolina.

3.4 Critical Source Areas

Table 2 gives the land area in CSAs by pollutant and land use. The area of CSAs for sediment is 31 ha, of which 24.5 ha is agricultural land and 5.6 ha are wetland. The total area of CSAs

for nitrogen is 2.5 ha, of which 1.8 ha are agricultural land and .6 ha are urban land. The total area of CSAs for phosphorus is 167.4 ha, of which 145.6 ha are agricultural land, 10 ha are urban land, and 11 ha are wetland. Figure 5 illustrates the location of CSAs for sediment, nitrogen, and phosphorus in the Neshanic River Watershed.

4 Conclusions

The pollutants generated in CSAs have a high potential of being transported to streams. Hence, targeting BMPs to CSAs is an ideal way to reduce NPS pollution. The ideal CSAs for targeting BMPs varies by pollutant. Without targeting, the potential area for implementing agricultural BMPs is 3628 ha, the total agricultural area in the watershed. The effectiveness and efficiency of lowering sediment loads in the watershed would be much higher by targeting agricultural BMPs to the 1291 ha of agricultural land classified as HSAs or the 121 ha of agricultural land classified as high potential sediment producing areas. Targeted area for BMPs for sediment reduction can be further reduced by applying BMPs to the 24 ha of CSAs for sediment identified in this study. Similarly, the targeted areas for implementing agricultural BMPs to reduce nitrogen pollution in the watershed can be reduced to 1291 ha based on HSAs, 8 ha based on high potential nitrogen producing areas or to 2 ha based on CSAs. Finally, the targeted area for implementing agricultural BMPs to reduce phosphorus pollution in the watershed can be reduced to 1291 ha based on HSAs, 627 ha based on high potential phosphorus producing areas, or 146 ha based on CSAs. Targeting BMP implementation to finer-scaled CSAs improves the effectiveness and economic efficiency of targeting. In addition, the final choice of targeted areas (i.e., HSAs, high potential pollution areas, or CSAs) depends on the desired amount of pollution reduction, which is an important consideration, for example, when implementing total maximum daily loads for pollutants.

Most existing methods for identifying CSAs are based on a single criterion, such as STIs or high pollution producing areas (Qiu 2009; Giri et al. 2012). A major contribution of this study is that it delineates CSAs for controlling sediment, nitrogen, and phosphorus pollution of streams in the Neshanic River watershed in New Jersey by integrating two criteria: HSAs identified using STIs; and high pollution producing areas identified using SWAT. Specifically, CSAs for sediment, nitrogen and phosphorus are identified by the intersection of HSAs and high potential pollution producing areas in the watershed. The advantage of using an integrated approach to delineate CSAs in the Neshanic River watershed is that it can significantly reduce the area targeted for BMP implementation, which would improve the economic efficiency of

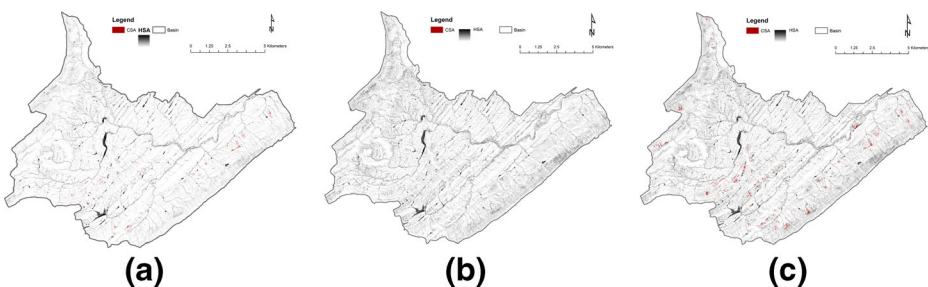


Fig. 5 Critical source areas for sediment (a), nitrogen (b), and phosphorus (c) in the Neshanic River watershed

targeting for NPS pollution reduction. Targeting BMPs to CSAs identified using the integrated approach described here can increase the economic efficiency of reducing NPS pollution.

This study used a threshold value of ten for STIs to define HSAs and applied the natural break procedure embedded in ArcGIS to define the high potential pollution producing areas. In practice, there are different ways to define HSAs based on STI and high pollution producing areas based on the pollutant loads simulated using SWAT, which are used to define CSAs in this study. Resource managers should use their local knowledge and understanding of pollution to select the most appropriate way to define HSAs and high pollution producing areas. The procedures described in this study provide one way to define HSAs, high pollution producing areas, and CSAs. This novel CSAs identification technique can be applied widely in watersheds where restoration funding is a constraint.

Although this study provides clear direction for targeting BMPs to CSAs, it is not clear how much water quality would be improved by targeting BMPs to CSAs vs. implementing BMPs based on other targeting criteria. Future research could install alternative BMPs both inside and outside of CSAs and empirically assess the extent and economic efficiency of pollution reduction with both approaches. Such research could be carried out either through experiments at a field scale or modeling at a larger watershed scale. Research results would improve the understanding of how pollution reduction efficacy and efficiency are influenced by the placement of BMPs and, perhaps, form the basis for developing various incentives and policies by land use planners and watershed managers to encourage agricultural producers to adopt BMPs in CSAs.

Acknowledgments The authors acknowledge the funding support by the USDA National Institute of Food and Agriculture through an Agriculture and Food Research Initiative Competitive Grant to New Jersey Institute of Technology (Grant Number 2012-67019-19348).

Compliance with Ethical Standards The project is partially supported by the U.S. Department of Agriculture National Institute of Food and Agriculture (Award #: 2012-67019-19348) to New Jersey Institute of Technology. The manuscript is an original contribution of all listed authors. There are no potential conflicts of interests or human/animal subject involvement. Proper acknowledgements to others have been made through the references.

References

- Ardon M, Montanari S, Morse JL, Doyle MW, Bernhardt ES (2010) Phosphorus export from a restored wetland ecosystem in response to natural and experimental hydrologic fluctuations. *J Geophys Res* 115(G4):1–12
- Arnold JG, Srinivasan R, Muttiah RS, Williams JR (1998) Large area hydrologic model development and assessment part 1: model development. *J Am Water Resour As* 34(1):73–89
- Brenning A (2007) RSAGA: SAGA geoprocessing and terrain analysis in R, available at: <http://cran.r-project.org/web/packages/RSAGA/index.html>. Accessed 24 July 2016.
- Buchanan BP, Archibald JA, Easton ZM, Shaw SB, Schneider RL, Walter MT (2013) A phosphorus index that combines critical source areas and transport pathways using a travel time approach. *J Hydrol* 486:123–135
- Buchanan BP, Fleming M, Schneider RL, Richards BK, Archibald J, Qiu Z, Walter MT (2014) Evaluating topographic wetness indices across central New York agricultural landscapes. *Hydrol Earth Syst Sc* 18(8): 3279–3299
- Carpenter SR, Caraco NF, Correll DL, Howarth RW, Sharpley AN, Smith VH (1998) Nonpoint pollution of surface waters with phosphorus and nitrogen. *Ecol Appl* 8(3):559–568
- Chen L, Qian X, Shi Y (2011) Critical area identification of potential soil loss in a typical watershed of the three gorges reservoir region. *Water Resour Manag* 25:3445–3463
- Costa-Cabral MC, Burges SJ (1996) Digital elevation model networks (DEMON): a model of flow over hillslopes for computation of contributing and dispersal areas. *Water Resour Res* 30(6):1681–1692

- Diebel MW, Maxted JT, Nowak PJ, Zanden MJV (2008) Land scape planning for agricultural nonpoint source pollution reduction I: a geographic allocation framework. *Environ Manag* 42(5):789–802
- Doody DG, Archbold M, Foy RH, Flynn R (2012) Approaches to the implementation of the water framework directives: targeting mitigation measures at critical source areas of diffuse phosphorus in Irish catchments. *J Environ Manag* 93(1):225–234
- Ghebremichael LT, Veith TL, Hamlett JM (2013) Integrated watershed and farm scale modeling framework for targeting critical source areas while maintaining farm economic viability. *J Environ Manag* 114:381–394
- Giri S, Nejadhashemi AP, Woznicki SA (2012) Evaluation of targeting methods for implementation of best management practices in the Saginaw River watershed. *J Environ Manag* 103:24–40
- Gupta HV, Sorooshian S, Yapo PO (1999) Status of automatic calibration for hydrologic models: Comparison with multilevel expert calibration. *J Hydrol Eng* 4(2):135–143
- Gyawali S, Techato K, Yuangyai C, Musikavong C (2013) Assessment of relationship between landuses of riparian zone and water quality of river for sustainable development of river basin, a case study of U-Tapao river basin, Thailand. *Prog Environ Sci* 17:291–297
- Hayakawa A, Shimizu M, Woli KP, Kuramochi K, Hatano R (2006) Evaluating stream water quality through landuse analysis in two grassland catchments: impact of wetlands on stream nitrogen concentration. *J water Qual Manage* 35(2):617–627
- Herron NF, Hairsine PB (1998) A scheme for evaluating the effectiveness of riparian zones in reducing overland flow to streams. *Aust J Soil Res* 36(4):683–698
- Hong B, Swaney D (2007) Generating maps of soil topographic index. Cornell University, Soil and Water Research Group Accessed 24 July 2016 Available at: <http://soilandwater.bee.cornell.edu/tools/STI.pdf>
- Horn BK (1981) Hill shading and the reflectance map. *P IEEE* 69:14–47
- Kaini P, Artita K, Nicklow JW (2012) Optimizing structural best management practices using SWAT and genetic algorithm to improve water quality goals. *Water Resour Manag* 26(7):1827–1845
- Kumar S, Mishra A (2015) Critical erosion area identification based on hydrological response unit level for effective sediment control in a river basin. *Water Resour Manag* 29(6):1749–1765
- Lyon SW, Ge'ard-Marcant P, Walter MT, Steenhuis TS (2004) Using a topographic index to distribute variable source area runoff predicted with the SCS-curve number equation. *Hydrol Process* 18(15):2757–2771
- Machiwal D, Madan KJ, Mal BC (2006) Modelling infiltration and quantifying spatial soil variability in a watershed of Kharagpur, India. *Biosyst Eng* 95(4):569–582
- Miller JD, Schoonover JE, Williard KWI, Hwang CR (2011) Whole catchment land cover effects on water quality in the lower Kaskaskia River watershed. *Water Air Soil Pollut* 221:337–350
- Moriyasi DN, Arnold JG, Van Liew MW, Binger RL, Harmel RD, Veith V (2007) Model evaluation guidelines for systematic quantification of accuracy in watershed simulations. *Trans ASABE* 50(3):885–900
- Nash JE, Sutcliffe JV (1970) River flow forecasting through conceptual models: part 1. A discussion of principles. *J Hydrol* 10(3):282–290
- NASS (2014) National Agricultural Statistics Service: CropScape-Cropland Data Layer Available at: <http://nassgeodata.gmu.edu/CropScape/>. Accessed 24 July 2016.
- NJDEP (2011) Surface water quality standards. NJAC 7:9B, Bureau of Water Quality Standards and Assessment, NJDEP, Trenton, NJ.
- Pandey A, Chowdary VM, Mal BC (2007) Identification of critical erosion prone areas in the small agricultural watershed using USLE, GIS and remote sensing. *Water Resour Manag* 21(4):729–746
- Pratt B, Chang H (2012) Effects of land cover, topography, and built structure on seasonal water quality at multiple spatial scales. *J Hazard Mater* 209:48–58
- Qiu Z (2009) Assessing critical source areas in watersheds for conservation buffer planning and riparian restoration. *Environ Manag* 44(5):968–980
- Qiu Z, Wang L (2014) Hydrological and water quality assessment in a suburban watershed with mixed land uses using the SWAT model. *J Hydrol Eng* 19(4):816–827
- Seibert J, McGlynn BL (2007) A new triangular multiple flow direction algorithm for computing upslope areas from gridded digital elevation models. *Water Resour Res* 43(4):W04501
- Shen Z, Hong Q, Chu Z, Gong Y (2011) A framework for priority non-point source area identification and load estimation integrated with APPI and PLOAD model in Fujiang watershed, China. *Agr water Manage* 98(6): 977–989
- Shen Z, Zhong Y, Huang Q, Chen L (2015) Identifying non-point source priority management areas in watersheds with multiple functional zones. *Water Res* 68:563–571
- Singh, J. Knapp HV, Demissie M (2004) Hydrologic modeling of the Iroquois River watershed using HSPF and SWAT. ISWS CR 2004–08. Champaign, Ill.: Illinois State Water Survey. <http://swat.tamu.edu/media/90101/singh.pdf>. Accessed 24 July 2016.
- Sivertun A, Prange L (2003) Non-point source critical area analysis in the Gisselo watershed using GIS. *Environ Model Softw* 18(10):887–898

- Srinivasan MS, McDowell RW (2009) Identifying critical source areas for water quality: 1. Mapping and validating transport areas in three head water catchments in Otago New Zealand. *J Hydrol* 379(1):54–67
- Thompson JJD, Doody DG, Flynn R, Watson CJ (2012) Dynamics of critical source areas: does connectivity explain chemistry? *Sci Total Environ* 435:499–508
- Trevisan D, Dorioz JM, Poulenard J, Quetin P, Combaret CP, Merot P (2010) Mapping of critical source areas for diffuse fecal bacterial pollution in extensively grazed watersheds. *Water Res* 44(13):3847–3860
- Tuppad P, Srinivasan R (2008) Bosque River environmental infrastructure improvement plan: phase II BMP modeling report. Publ. No. TR-313 College Station, TX: Texas A&M Univ., Texas AgriLife Research.
- USEPA (2009) National water quality inventory: Quality of our nation's water: report to congress 2004 reporting cycle. EPA 841-R-08-001. US Environmental Protection Agency, Office of Water, Washington DC.
- Walter MT, Walter MF, Brooks ES, Steenhuis TS, Boll J, Weiler K (2000) Hydrologically sensitive areas: Variable source area hydrologically implications for water quality risk assessment. *J Soil Water Conserv* 55(3):277–284
- Wan R, Cai S, Li H, Yang G, Li Z, Nie X (2014) Inferring landuse and land cover impact on stream water quality using a Bayesian hierarchical modeling approach in the Xitiaoxi river watershed China. *J Environ Manag* 133:1–11
- Wang L, Liu H (2006) An efficient method for identifying and filling surface depressions in digital elevation models for hydrologic analysis and modelling. *Int J Geogr Inf Sci* 20(2):193–213
- White MJ, Storm DE, Busted PR, Stoodley SH, Phillips SJ (2009) Evaluating nonpoint source critical source area contributions at the watershed scale. *J Environ Qual* 38(4):1654–1663
- Wilson C, Weng Q (2010) Assessing surface water quality and relation with urban land cover changes in the Lake Caumet area, greater Chicago. *Environ Manag* 45(5):1096–1111
- Zampella RA, Procopio NA, Lathrop RG, Dow CL (2007) Relationship of landuse/land-cover patterns and surface water quality in the Mullica River basin. *J Am Water Resour Assoc* 43(3):594–604
- Zhou H, Gao C (2011) Assessing the risk of phosphorus loss and identifying critical source areas in the Chaohu Lake watershed, China. *Environ Manag* 48(5):1033–1043